Korean J. Chem. Eng., **16**(6), 764-773 (1999)

Stability Analysis of Heated Thin Liquid-Film Flows with Constant Thermal Boundary Conditions

Hyo Kim†

Department of Chemical Engineering, University of Seoul, 90 Jeonnong-Dong, Dongdaemun-Gu, Seoul 130-743, Korea
(Received 21 June 1999 • accepted 3 September 1999)

Abstract–To answer the questions on the behavior of liquid flows under complicatedly combined actions of stresses, evaporation and temperature-dependent surface tension effects, thin liquid layers flowing under gravity down an inclined plane uniformly heated from below are considered. There may be two thermal boundary conditions on the hot plate, i.e., either constant heat flux or fixed temperature. By using long-wave approximation, the nonlinear evolution equations governing the two-dimensional surface waves have been derived upto $O(\varepsilon^2)$ and $O(\varepsilon)$ for the constant heat flux and the fixed temperature case, respectively. Here the small parameter $\varepsilon(<<1)$ is the ratio of the characteristic length scale parallel to the flow to the initial basic film thickness. The linear and the nonlinear stability analyses are also performed by using numerical calculations. Consequently, the flow subjected to the constant heat flux can be marked as a more stable system than the flow mechanism at a fixed-temperature boundary condition.

Key words: Thin Liquid-Film Flow, Constant Heat Flux, Fixed Temperature, Long-wave Approximation, Stability

INTRODUCTION

Thin liquid film has attracted much attention in many contexts, such as the cooling of the thin liquid film radiator, gas turbine blade tips, rocket engines, microelectronics arrays and hot fuel surfaces in nuclear reactors due to its high heat and mass transfer rates in comparison with the volume of throughflow. Considering the effectiveness of the heat removal rates in the equipments the film has to be kept as thin as possible. However, the thin film flow is subject to competing instabilities prior to actual rupture which will form dry regions resulting in possible overheating the wall of the operating equipments. For the application purposes we need to explore the characteristics of non-isothermal thin liquid film flows involving the combined effects of evaporation, temperature-dependent surface tension and stresses. Usually, one of the two specific boundary conditions in temperature, i.e., constant wall temperature and constant heat flux, is employed to the solid wall through which heat is transferred to the above liquid layer. Here we will investigate thin liquid films draining under gravity down an inclined plane which are uniformly heated from below with constant thermal boundary conditions. The liquid may be nonvolatile or volatile.

Flowing liquid film is always susceptible to instability as the mean flow rates increase and traveling waves appear on the free surface whether the system is isothermal or not. The study of the thin liquid layers flowing under a gravitational force down an inclined isothermal plane surface was initiated by Benjamin [1957] and Yih [1963]. They identified regimes of linear stability as a function of the Reynolds number and the superimposed wavenumber. It was found the stability region gets smaller as Reynolds number increases, and around cutoff wavenumber the exponentially growing wave develops into the almost sinusoidal permanent traveling wave with small but equilibrium amplitude. Since that time quite a number of extensions of the isothermal case have been made by several authors, i.e., Benny [1966], Gjevik [1970], Lin [1974], Chang [1989], and Kim et al. [1992, 1993, 1994, 1997], to name only a few. Benny [1966] and Gjevik [1970] extended this case to the nonlinear regime and derived a nonlinear evolution equation for the film thickness. Lin [1974] showed the side-band stability near the neutral curve and found out the supercritical region by weakly nonlinear analysis. Chang [1989] used an advanced bifurcation theory to study all types of steady wave solutions with a phase speed close to the interfacial velocity. For a modern application of the thin film flow to design an advanced space radiator, Kim et al. [1992, 1993, 1994] examined the interaction of an electrostatic field on a flowing liquid-metal film on a plane of inclined surface, inside a rotating cone and a cylindrical surface. The electrostatic field exerts a tensile force on the liquid film, pulling it away from a puncture probably made in the radiator shell due to micrometeorite impacts in space. Kim [1997] also performed a long-wave analysis of the film flow under an electrostatic field to explain the questions concerning the nonlinear instabilities.

If the plane surface occupied by a thin liquid layer is heated with a constant hot temperature, the results of heat transfer appear mainly in thermocapillary and vapor recoil effects. To consider these effects quantitatively, Burelbach et al. [1988] examined the nonlinear stability of evaporating/condensing liquid layer rested on a flat plane through which heat was transferred. They formulated the two-phase problem upto $O(\varepsilon)$ using the one-sided model with assumptions that density, viscos-

†To whom correspondence should be addressed.
E-mail: hkim@uoscc.uos.ac.kr

ity, and thermal conductivity were all much greater in the liquid than in the vapor. Their mechanism included the effects of mass loss due to evaporation, vapor recoil, thermocapillarity and van der Waals force acting as a negative disjoining pressure on the rupturing film. The long-wave instabilities of heated falling films in the absence of the van der Waals force were studied by Joo et al. [1991]. They extended the research of Burelbach et al. [1988] to contain the inertial effect of mean flow due to gravity, and they employed a boundary condition of constant temperature into the film flow and analyzed the free-surface instability upto O(ε). They answered the question of how the free surface evolves in advance of actual rupture. A monochromatic wave with an initial small disturbance may develope into a single finger downward upon heating a thin liquid layer. The downward growth slows because of the proximity of the bottom wall, and the tip of the single finger gets flattened. The result is that the fingertip splits and two downward fingers are made. Eventually, this produced two dry spots according to the two-dimensional lubrication theory.

The aim of the present work is to address the questions concerning the stability of an evaporating thin liquid film heated with either a constant heat flux or a fixed temperature. For a constant heat flux case a nonlinear evolution equation for the film thickness has been derived upto (ε^2), at which the onset of the vapor recoil and thermocapillarity effects can be observed. However, for a fixed temperature these effects appear from O (ε) and thus it is enough to have an evolution equation upto this order of magnitude. Since the layer is assumed very thin for both cases, the temperature profiles are expected to be linear with the film depth in the lowest order due to the effect of a thermal conduction. The van der Waals force is not included in this problem. From the acquired evolution equations the linear stability analysis is performed about the uniformly evaporating flat film. The nonlinear behavior of disturbances is also investigated by a numerical computation using a Fourier-spectral method.

The following sections are composed of formulation, thin film limit, linear stability analysis, nonlinear film evolution and conclusions. In the section of formulation, the flow configuration and governing equations in both of liquid and vapor phases are explained. The section of thin film limit shows the asymptotic approaches to the governing equations to get a nonlinear evolution equation for the film height. From the transient, spatially uniform and basic state, linear stability analysis has been performed by introducing a small disturbance into the free surface in the section of linear stability analysis. The various nonlinear stabilities are computed in the section of nonlinear film evolution, and in the final section the results are concluded.

FORMULATION

For the investigation of the effects of heat transfer to the thin liquid film as it flows down an inclined plane uniformly heated below, two kinds of thermal boundary conditions can be applied to the plane wall as a constant heat flux q_c or a fixed temperature T_H. Here both boundary conditions are taken into account. As a more general approach the fluid is assumed as a volatile liquid in this mathematical formulation. That is, if we consider the nonvolatile case, then just omitting the evaporation factor will automatically generate the aimed equations. The liquid is treated as an incompressible, viscous fluid with constant physical properties except the surface tension σ, which is usually decreased with temperature T. The plane is assumed to make an angle β with the horizontal, and with the two-dimensional coordinate system the x axis is parallel to the plane, while the y axis is perpendicular to it (Fig. 1). It means that the components of the gravitational acceleration g in the x and y directions are g sin β and −g cos β, respectively. The liquid layer is bounded above by its vapor with a saturation temperature T_s and laterally unbounded. The liquid-vapor interface is defined by h(t, x), which is a function of the lateral coordinate x and time t.

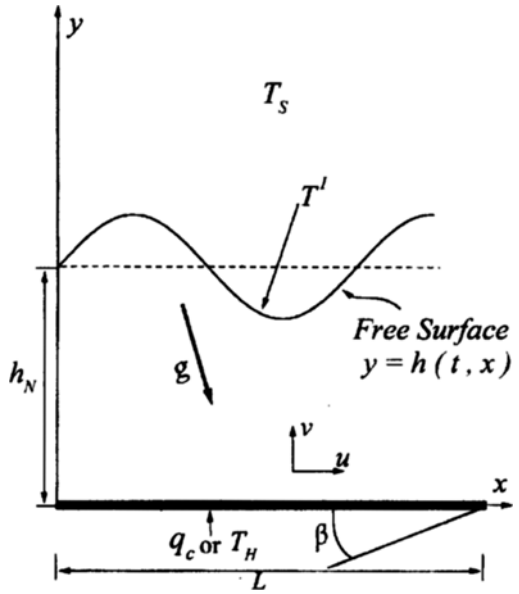

Fig. 1. The physical configuration for a heated thin liquid-film flows with constant thermal boundary conditions.

The liquid layer is governed by the incompressible Navier-Stokes and energy equations. Suppose that we define h_N as the characteristic thickness which is the initial value of the flat layer and

$$\varepsilon = h_N/L \ll 1, \quad (1)$$

where L is the characteristic length scale parallel to the x axis. We assume the film is thin relative to the expected length scale of the disturbances in the y direction. From now the nondimensionalized governing equations and boundary conditions are introduced. However, one has to be cautious before proceeding because for the two proposed thermal boundary conditions there have to be two different scaling thermal units according to either the temperature or the flux conditions. For convenience' sake, only q_c will be employed for both cases. If the boundary condition is a constant temperature, then it is enough to take $k\Delta T/h_N$ instead of q_c. Here k is the thermal conductivity of the liquid and $\Delta T = T_H - T_s$. By letting h_N be the unit of length in the y direction, L the unit of length in x di-

rection, u_N the unit of velocity in the x direction (it will be chosen later.), εu_N the unit of velocity in the y direction, L/u_N the unit of time, ρu_N^2 the unit of pressure p (ρ is the liquid density), $q_c h_N/k$ the unit of temperature difference ($T-T_s$), q_c/L_h the unit of mass flux J due to the evaporation (L_h is the latent heat of evaporation), we have determined the dimensionless equations of motion and energy. The continuity equation is

$$u_x+v_y=0, \tag{2}$$

while the x and y components of the momentum equation are

$$\varepsilon(u_t+uu_x+vu_y)=-\varepsilon p_x+\frac{1}{Re}(\varepsilon^2u_{xx}+u_{yy})+\frac{\sin\beta}{Fr^2}, \tag{3}$$

and

$$\varepsilon^2(v_t+uv_x+vv_y)=-p_y+\frac{\varepsilon}{Re}(\varepsilon^2v_{xx}+v_{yy})-\frac{\cos\beta}{Fr^2}. \tag{4}$$

The energy equation is reduced to

$$\varepsilon(T_t+uT_x+vT_y)=\frac{1}{RePr}(\varepsilon^2T_{xx}+T_{yy}), \tag{5}$$

in which Re is the Reynolds number ($=u_N h_N/\nu$), Fr the Froude number ($=u_N/\sqrt{gh_N}$) and $Pr=\nu/\kappa$ as the Prandtl number. ν is the kinematic viscosity and κ is the thermal diffusivity. The subscripts represent the partial derivatives.

To solve the governing equations we must still give the boundary conditions. Along the solid plane wall, y=0, we have the boundary conditions

$$u=v=0 \text{ and } \begin{cases} T_y=-1 \text{ for a constant heat flux} \\ \text{or} \\ T=1 \text{ for a fixed temperature.} \end{cases} \tag{6}$$

On the fluid interface, y=h(t, x), we have the jump mass condition

$$\frac{EJ}{Re}=\frac{\varepsilon(v-uh_x-h_t)}{(1+\varepsilon^2h_x^2)^{1/2}}, \tag{7}$$

the tangential and the normal stresses [Delhaye, 1974] are, respectively,

$$\begin{aligned}&(u_y+\varepsilon^2v_x)(1-\varepsilon^2h_x^2)-4\varepsilon^2h_xu_x\\&\quad-\left(\frac{\mu^v}{\mu}\right)\{(u_y^v+\varepsilon^2v_x^v)(1-\varepsilon^2h_x^2)-4\varepsilon^2h_xu_x^v\}\\&\quad=-2\varepsilon\frac{M}{Pr}(T_x+h_xT_y)(1+\varepsilon^2h_x^2)^{1/2},\end{aligned} \tag{8}$$

$$\begin{aligned}&\left(1-\frac{3}{2D}\frac{1}{D}\right)\frac{E^2J^2}{Re^2}+p-p^v-\frac{2}{Re}\varepsilon(1+\varepsilon^2h_x^2)^{-1}[\varepsilon^2h_x^2u_x\\&\quad-h_x(u_y+\varepsilon^2v_x)+v_y-\left(\frac{\mu^v}{\mu}\right)\{\varepsilon^2h_x^2u_x^v-h_x(u_y^v+\varepsilon^2v_x^v)+v_y^v\}]\\&\quad=-\varepsilon^2\frac{We(1-CT)h_{xx}}{(1+\varepsilon^2h_x^2)^{3/2}},\end{aligned} \tag{9}$$

and the jump energy condition becomes

$$\begin{aligned}&J\left[1+\left(1-\frac{4}{9}D^2\right)\frac{E^2J^2}{D^2\Lambda}\right]+\left[-\varepsilon^2h_xT_x+T_y-\left(\frac{k^v}{k}\right)(-\varepsilon^2h_xT_x^v+T_y^v)\right]\\&(1+\varepsilon^2h_x^2)^{-1/2}+\frac{16}{9}\frac{\varepsilon Re}{\Lambda}\frac{J}{(1+\varepsilon^2h_x^2)}[\varepsilon^2h_x^2u_x\\&-h_x(u_y+\varepsilon^2v_x)+v_y-\frac{3}{2D}\frac{1}{D}\left(\frac{\mu^v}{\mu}\right)\{\varepsilon^2h_x^2u_x^v-h_x(u_y^v+\varepsilon^2v_x^v)+v_y^v\}]=0.\end{aligned} \tag{10}$$

Here the superscript v represents the properties of the vapor phase and we have introduced the evaporation number $E=q_c h_N/(\rho\nu L_h)$, the ratio of density of between liquid and vapor $D=(3/2)(\rho^v/\rho)$, the Weber number $We=\sigma_0/(\rho U_N^2 h_N)$, the capillary number $C=\gamma q_c h_N/(\sigma_0 k)$, the Marangoni number $M=\gamma q_c h_N/(2\rho\kappa u_N k)$, and the dimensionless latent heat of vaporization $\Lambda=(8/9)(h_N^2L_h)/\nu^2$. The surface tension σ is assumed to decrease linearly in temperature, i.e., $\sigma=\sigma_0-\gamma(T^I-T_s)$, where σ_0 is the surface tension at the saturation temperature, γ is the temperature gradient of σ (generally γ is positive) and T^I is the local temperature on the interface. To derive the shear stress condition (8), we assumed a no-slip at the interface between the liquid and vapor phases. Finally, we need another boundary condition to relate the mass loss to the temperature difference between at the free surface and vapor space, that is, a constitutive equation [Palmer, 1976]

$$KJ=T. \tag{11}$$

The K is the degree of non-equilibrium at the vaporizing surface and defined by

$$K=\left(\frac{kT_s^{3/2}}{\alpha_{ac}h_N\rho^vL_h^2}\right)\left(\frac{2\pi R_g}{M_w}\right)^{1/2}, \tag{12}$$

where α_{ac} is the accommodation coefficient, R_g is the universal gas constant and M_w is the molecular weight.

In case of the nonvolatile layer, i.e., E=0, we need another boundary condition at the free surface for the heat removing to the vapor phase. Since there is no mass flux, i.e., J=0, we have to combine (10) with the last term neglected and (11) to keep the jump energy balance valid. Here, the K is no more defined by (12) and K^{-1} becomes a Biot number.

The additional conditions are the appropriate initial conditions for the film thickness, velocity and temperature fields.

THIN FILM LIMIT

With the help of thin film limit, $\varepsilon \ll 1$, of (2)-(11) nonlinear evolution equations for the film depth h(t, x) to the two cases of thermal boundary conditions will be derived in this section. To formulate this two-phase flow problem more tractably, one can use the one-sided model [Burelbach et al., 1988], i.e., the density, viscosity and conductivity of the liquid phase is treated much greater than those in the vapor phase. However, the term of vapor density multiplied by vapor velocity is retained because its value might be large.

Assuming that the Reynolds number is order unity, a similar analysis for an isothermal thin film flowing down an inclined plane has been performed by several authors. The other parameters are taken to have some proper magnitudes to retain the physical effects, i.e., $E=O(\varepsilon)$, $D=O(\varepsilon^2)$, $We=O(\varepsilon^{-2})$, $\Lambda=O(\varepsilon^{-4})$, $Fr=O(1)$, $KM=O(1)$ and $Pr=O(1)$. The order of magnitudes are reasonable in the liquids such as water at 1 atm. In order to apply a regular perturbation method to (2)-(11), we expand the dependent variables in small ε:

$$u = u_0+\varepsilon u_1+\varepsilon^2 u_2\cdots, \quad (13)$$

$$v = v_0+\varepsilon v_1+\varepsilon^2 v_2\cdots, \quad (14)$$

$$T = T_0+\varepsilon T_1+\varepsilon^2 T_2\cdots, \quad (15)$$

$$J = J_0+\varepsilon J_1+\varepsilon^2 J_2\cdots, \quad (16)$$

$$p = p_0+\varepsilon p_1+\varepsilon^2 p_2\cdots, \quad (17)$$

Substituting (13)-(17) into (2)-(11), expanding all dependent variables in a power series in ε, and finally we can obtain the desired equations for the first two and three orders in ε according to the boundary conditions of the fixed temperature and the constant heat flux, respectively. During the calculation the vapor pressure has been neglected.

1. At a Constant Heat Flux Condition

After substituting the calculated results of u(t, x, h), v(t, x, h) and J(t, x) accurate to $O(\varepsilon^3)$ into the jump mass condition (7), we can derive the nonlinear evolution equation in the film depth h(t, x) upto $O(\varepsilon^2)$, i.e.,

$$h_t+\frac{\bar{E}}{Re}\left[1+EPrh+E^2KPr^2(h+h^2)-\frac{E^2}{D^2\Lambda}\right]$$
$$+[A(h)+B(h)h_x+C(h)h_{xx}+D(h)h_{xxx}+E(h)h_{xxxx}+F(h)h_x^2]_x$$
$$+\varepsilon^4\frac{\sin\beta}{Fr^2}Re^3We\left(\frac{8}{5}h^5h_x^2h_{xx}+\frac{4}{5}h^6h_{xx}^2+\frac{9}{8}h^6h_xh_{xxx}\right)_x=0, \quad (18)$$

where

$$A(h)=\frac{\sin\beta Re}{3Fr^2}h^3+\frac{\sin\beta Re}{8Fr^2}E\left(Pr+\frac{5}{3}\right)h^4+\frac{\sin\beta Re}{Fr^2}E^2$$
$$\left\{\left(\frac{5}{24}-\frac{3}{40}Pr+\frac{19}{60}Pr^2\right)h+\frac{13}{24}KPr^2\right\}h^4,$$

$$B(h)=\varepsilon\frac{Re}{3Fr^2}\left(\frac{2\sin^2\beta Re^2}{5Fr^2}h^3-\cos\beta\right)h^3$$
$$+\varepsilon^2\bar{E}\left(\frac{1}{Re}h-KMh^2-\frac{E^2Pr}{DRe}h^3+\frac{\cos\beta Re}{8Fr^2}Prh^4-\frac{5}{24}\frac{\cos\beta Re}{Fr^2}h^4\right.$$
$$+\frac{\sin^2\beta Re^3}{3Fr^4}KPr^2h^6+\frac{11}{72}\frac{\sin^2\beta Re^3}{Fr^4}Pr^2h^7-\frac{7}{144}\frac{\sin^2\beta Re^3}{Fr^4}Prh^7$$
$$\left.+\frac{1667}{5040}\frac{\sin^2\beta Re^3}{Fr^4}h^7\right),$$

$$C(h)=\varepsilon^2\frac{\sin\beta Re}{Fr^2}\left(\frac{3}{4}-\frac{Re}{2}KMh-\frac{E^2Pr}{2D}h^2-\frac{5}{56}\frac{\cos\beta Re^2}{Fr^2}h^3\right.$$
$$\left.+\frac{1}{28}\frac{\sin^2\beta Re^4}{Fr^4}h^6\right)h^4,$$

$$D(h)=\varepsilon^3WeRe\left\{\frac{1}{3}h^3-\frac{1}{8}E\left(Pr-\frac{5}{3}\right)h^4\right\},$$

$$E(h)=\frac{5}{56}\varepsilon^4\frac{\sin\beta Re^3}{Fr^2}Weh^7,$$

$$F(h)=\varepsilon^2\frac{\sin\beta Re}{Re^2}\left(\frac{7}{3}-\frac{3}{2}KMReh-\frac{3E^2Pr}{2D}h^2\right.$$
$$\left.-\frac{13}{40}\frac{\cos\beta Re^2}{Fr^2}h^3+\frac{149}{630}\frac{\sin^2\beta Re^4}{Fr^4}h^6\right)h^3, \quad (19)$$

where $\bar{E}=E/\varepsilon=O(1)$. The evolution equation is a parabolic partial differential equation and the solution-seeking procedure will be addressed later. In (18) and (19), the terms proportional to E describe the effect of evaporation. If the layer is nonvolatile, i.e., E=0, the accumulated heat in the liquid phase will be transferred into the gas phase by the Newton's law of cooling, and thus J is no more evaporating mass flux and it becomes a heat flux removing through the free surface. The temperature profile have the same forms as in the volatile case except that K represents an inverse Biot number. From (18), we find the thermal effects such as thermocapillarity and vapor recoil occur from the terms of order ε^2.

2. At a Fixed Temperature Condition

Using the same procedures as in the constant heat flux case we can get the results of u(t, x, h), v(t, x, h) and J(t, x) upto O (ε). Since all of the thermal effects such as thermocapillarity, vapor recoil and mass loss are included in this order, it is not necessary to proceed to the next second order of ε^2 like the previous subsection. Plugging the acquired velocity profiles and mass flux at the interface into the jump mass balance, the nonlinear evolution for the film depth accurate to (ε^2) has the form:

$$h_t+\frac{\sin\beta Re}{Fr^2}h^2h_x+\frac{\bar{E}}{Re}\frac{1}{(K+h)}\left(1+\frac{EPr}{3}\frac{h^3}{(K+h)^3}\right)$$
$$-\frac{\sin\beta Re}{120Fr^2}\frac{EPrh^4h_x}{(K+h)^3}(15K-7h)+(\bar{B}(h)h_x+\bar{D}(h)h_{xxx})_x=0, \quad (20)$$

where

$$\bar{B}(h)=\varepsilon\left(\frac{2}{15}\frac{\sin^2\beta Re^3}{Fr^4}h^6+\frac{1}{2}\frac{E^2}{DRe}\frac{h^3}{(K+h)^2}\right.$$
$$\left.-\frac{1}{3}\frac{\cos\beta Re}{Fr^2}h^3+\frac{KM}{Pr}\frac{h^2}{(K+h)^2}\right),$$

$$\bar{D}(h)=\frac{1}{3}\varepsilon^3WeReh^3. \quad (21)$$

Here the evaporation number $\bar{E}=E/\varepsilon=\frac{k\Delta T}{\varepsilon\mu L_h}=O(1)$, $E^2/D=O(1)$ and the Marangoni number $KM/Pr=\frac{K\gamma\Delta T}{2\mu u_N}=O(1)$. From (20) we can see the thermal parameters appear in O(ε) whereas they are included in $O(\varepsilon^2)$ for the case of fixed heat-flux heating problem.

LINEAR STABILITY ANALYSIS

Linear stability for an isothermal liquid film flowing down an inclined plane was studied by Benjamin [1957] and Yih [1963]. In the long wave limit their result is that the liquid film is stable if

$$Re<\frac{5}{6}\cot\beta. \quad (22)$$

When the liquid layer is artificially perturbed, two types of waves are observed. The first one is the nearly periodic surface wave and the other is a single wave with a large wave length compared with the amplitude. During the formation of these waves it is interesting to study the evolution of the waves initially excited in a small amplitude as time marches. The growth rate can be predicted by the linear stability analysis while the waves propagate downstream. When the flowing layer is isothermal the surface tension and the hydrostatic pressure act as stable factors whereas the mean shear flow makes the film unstable. The aim here is to expand the isothermal result to in-

clude the thermal effects given at the bottom wall. In order to perform the linear stability analysis a basic state has to be sought. Since the heated film is evaporating, the basic state will be a function of time. Hence letting $h_0(t)$ represent the basic state of h(t, x) and $\delta\eta(t, x)$ the perturbation of h(t, x) from the uniformly evaporating layer, i.e., $h=h_0+\delta\eta$, where δ is a small disturbance amplitude, we can derive the linearized basic state and disturbance equations from (18) and (20) for the constant heat flux and the fixed temperature cases, respectively. By plugging $h=h_0+\delta\eta$ into the evolution equations and expanding them in powers of δ, we can get the basic states from order one in δ and then the disturbance equations from $O(\delta)$. From the first order of δ, linearized disturbance equations can be acquired in η representing the perturbation of h from the basic state. To apply the linear stability analysis, η is assumed to have a time harmonic solution, i.e., $\eta=\exp[i(\alpha x-ct)]$, where α is the real wavenumber of the disturbance and $c=c_r+ic_i$ is the complex frequency. If c_i is negative, the flow is linearly stable, while if c_i is positive, the flow becomes unstable.

1. At a Constant Heat Flux Condition

The basic state equation describing the constant heat flux problem is easily obtained from (18) by setting $\frac{\partial}{\partial x}=0$:

$$\frac{dh_0}{dt}+\frac{\bar{E}}{Re}+(1+EPrh_0)+\frac{\bar{E}}{Re}E^2\left(KPr^2h_0+Pr^2h_0^2-\frac{1}{D^2\Lambda}\right)=0. \quad (23)$$

To solve the above equations we need an initial condition $h_0(0)=1$. If the terms of $O(\varepsilon^2)$ is neglected in (23), it is seen the basic state is calculated by analytical methods. After substituting the normal mode of $\eta=\exp[i(\alpha x-ct)]$ into the linearized equations of (18) and (19) about $h=h_0$, one obtains the stability results,

$$c_i=-\frac{\bar{E}}{Re}(E^2KPr^2+2E^2Pr^2h_0+EPr)+\alpha^2B_0-\alpha^4D_0, \quad (24)$$

$$c_r=\alpha\frac{\sin\beta Re}{Fr^2}\left[Pr^2E^2\left(\frac{13}{6}K+\frac{19}{12}h_0\right)h_0^3-PrE\left(\frac{1}{2}-\frac{3}{8}Eh_0\right)h_0^3+\left(\frac{25}{24}E^2h_0^2+\frac{5}{6}Eh_0+1\right)h_0^2\right]-\alpha^3C_0+\alpha^5\varepsilon_0, \quad (25)$$

where B_0, C_0, D_0 and E_0 denote the first order expansion coefficient in (19) about $h=h_0$, i.e., $B_0=B(h_0)$, $C_0=C(h_0)$, $D_0=D(h_0)$ and $E_0=E(h_0)$. The imaginary part of c in (24) states the onset of instability and shows the effective growth-rate terms, which are proportional to the wavenumber. The cutoff wavenumber α_c is calculated by setting $c_i=0$ in (24) and the wavenumber at the maximum growth rate α_m can be obtained as

$$\alpha_m=\frac{1}{\sqrt{2}}\sqrt{\frac{B_0}{D_0}}. \quad (26)$$

The linear phase velocity is given from the real part of c divided by α i.e., c_r/α. Here one can see the linearly unstable zone gets smaller in this constant heat flux problem as time elapses (see Fig. 2) because the mean flow rate decreases due to the evaporation and still more the thermocapillarity and vapor recoil acts as stabilizing factors at the same time. These phenomena can be promptly checked from B_0 in (24).

2. At a Fixed Temperature Condition

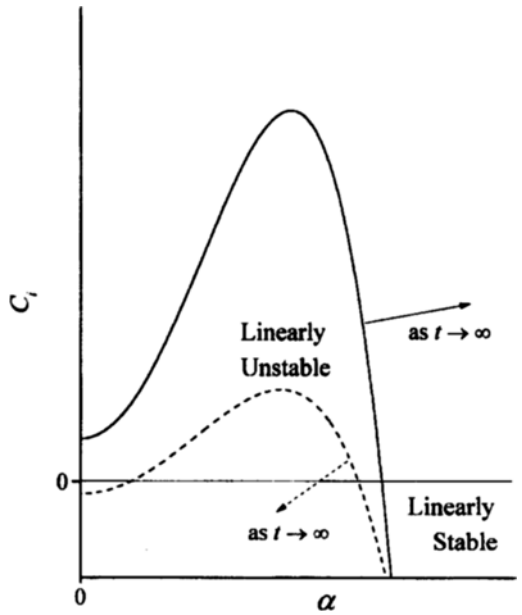

Fig. 2. Neutral stability curves in (α–c_i) domain describing the constant wall-temperature model (———) and the fixed flux model (----------).

The basic state solution of the film thickness calculated from (20) is given by

$$\frac{dh_0}{dt}+\frac{\bar{E}}{Re}\frac{1}{K+h_0}+\frac{1}{3}\varepsilon\frac{\bar{E}^2Pr}{Re}\frac{h_0^3}{(K+h_0)^4}=0. \quad (27)$$

With the same procedure as in the previous subsection the linear stability results for the fixed temperature case are calculated from (20) and (21) after these are linearized around $h=h_0$:

$$c_i=\frac{\bar{E}}{re}\frac{1}{(K+h_0)^2}-\frac{1}{3}\frac{\bar{E}E}{Re}Prh_0^2\frac{3K-h_0}{(K+h_0)^5}+\alpha^2\bar{B}_0-\alpha^4\bar{D}_0, \quad (28)$$

$$\alpha_r=\alpha\frac{\sin\beta Re}{Fr^2}\frac{h_0^2}{(K+h_0)^3}\left[EPrh_0^2\left(\frac{7}{120}h_0-\frac{1}{8}K\right)+K\left(K^2+\frac{5}{6}EKh_0+3h_0\right)+Kh_0^2\left(\frac{35}{24}E+3\right)+h_0^3\left(\frac{5}{8}E+1\right)\right]. \quad (29)$$

Here $\bar{B}_0$ and $\bar{D}_0$ are the values of $\bar{B}(h)$ and $\bar{D}(h)$ at $h=h_0$, respectively. The cutoff wavenumber α_c is obtained from $c_i=0$ in (28) and the maximum-growth-rate wavenumber α_m is yielded by calculating $dc_i/d\alpha=0$,

$$\alpha_m=\frac{1}{\sqrt{2}}\sqrt{\frac{\bar{B}_0}{\bar{D}_0}}, \quad (30)$$

and c_r/α stands for the phase speed of the moving interface. Referring to the neutral stability curve of c_i vs. α in Fig. 2, the thinning process developed by mass loss makes the flow system more unstable than at the condition of constant heat flux because of the combined destabilizing effects of thermocapillarity and vapor recoil. In addition, without the mass loss due to the evaporation only the thermocapillary effect plays an important role of thermal instability. However, in the constant heat flux problem the linear stability of the layer behaves like that of an isothermal problem in case of no evaporation, that is, the thermocapillarity does not affect the stability as we can

see by letting E=0 in (24). The similar behavior has been also observed by Burelbach et al. [1988] in the evaporating/condensing liquid layer rested on a flat plane, where there was no mean flow.

NONLINEAR FILM EVOLUTION

The linear stability analysis is only correct while the perturbed surface has a long wave length compared with its amplitude. However, as the linear wave evolves into the downstream it is modified by the nonlinear effects and the linear analysis is not valid any more. Thus to investigate the nonlinear effects on the surface wave the derived nonlinear evolution equations of (18) and (20) have to be solved numerically. The nonlinear equation depicting the film variations in an isothermal flow system was analytically solved by Gjevik [1970] and Lin [1974], etc. Gjevik [1970] examined the wave having a wavenumber close to the cutoff value by using a fundamental mode. Lin [1974] performed a weakly nonlinear analysis near the critical Reynolds number and found a transition point separating (α–Re) domain into a supercritical and a subcritical regions. Joo et al. [1991] and Kim [1997] solved the nonlinear evolution equation numerically by a Fourier-spectral method. Joo et al. [1991] examined the instabilities of heated falling films upto $O(\varepsilon)$ with a constant wall temperature and Kim [1997] calculated the isothermal film behavior under the influence of an electrostatic field. The initially computed surface-wave instability was coincided with the result from the linear stability analysis. They also showed the nonlinear modal interactions between the harmonics with higher frequencies.

The evolution equations of (18) and (20) are parabolic partial differential equations and one needs a initial value in the laterally unbounded domain. As an initial wave shape, a sinusoidal disturbance of small amplitude has been chosen to confirm the validity of the surface-wave developments as predicted by linear theory:

$$h(0, x) = 1 - 0.1\cos(\alpha x). \tag{31}$$

It makes the computational domain spatially periodic. To solve the evolution equations numerically a Fourier-spectral method is useful, i.e., the layer thickness h(t, x) is calculated by a finite Fourier series :

$$h(t, x) = \sum_{n=-N}^{n=N} a_n(t)\exp(i\alpha n x) + \text{complex conjugate} \tag{32}$$

with $N \geq 2^5$. The computational domain is set to $-\pi/\alpha \leq x \leq \pi/\alpha$. The solution for the time is calculated by a fourth-order modified Hamming's predictor-corrector method with the maximum tolerance of 10^{-12} using the fourth-order Runge-Kutta method for some initial predicting values. The evolution of the interface has been computed at the two thermal boundary cases with or without the effect of evaporation in order to check the stability behavior as predicted in the linear theory. For the computation the small parameter ε is set 0.05 to meet the assumed long wave approximation and the other ones are selected as $\bar{E} = 0.5$ (for the evaporation instance), Pr=1.0, Fr^2=0.2, $\bar{D} = 0.1$, K=0.2, M=100, and We=5, for the exemplary simulations. Here the characteristic velocity is defined as a viscous scale $u_N = \nu/h_N$. Hence the Re becomes one and $\sin\beta/Fr^2$ will be a new Reynolds number. The slant angles of the plane can be arbitrarily adopted in the derived evolution equations to consider the effects of the gravity, that is, if β=0 the fluid is the horizontal static layer and then increasing the angle the layer starts to move into the downstream. In the following subsections the numerical results will show different physical effects and their interactions to the applied thermal boundary conditions. These calculations are not necessarily physically realistic and just show the nondimensional parametric results.

1. At a Constant Heat Flux Condition

To examine the surface-wave configurations with a heat flux kept constant at the plane wall the evolution equation (18) has been solved with or without the effect of evaporation. First, with the mass loss included, i.e., $\bar{E} = 0.5$, the numerical calculations are performed as the inclination angle changes such as β=0, β=15° and β=30°. In this geometry and physical properties there is no wavenumber making the layer unstable, i.e., any imposed wavenumber will render the disturbed surface wave flat. Thus, with α=0.8 as an initial imparting disturbance wavenumber the evaporating layer becomes stable because this wavenumber locates in the stable region. Fig. 3(a) shows the surface-wave stability in the horizontal static layer. The film gets thinning and the depth between the crest and the trough becomes smaller and finally it ruptures at t_R=1.7869. This behavior can be easily explained with the evolution of the spectral coefficients in Fig. 3(b). The fundamental harmonics are linearly decayed at the initial point, which meets well the linear stability analysis, whereas the lower harmonics are slightly excited which means the initial simple harmonic function starts to break into a distorted harmonic wave with a little higher frequency. With β=15° and β=30°, the stability aspects are different from the static case. As the slant gets larger the surface-wave deformations become more severe as seen in Fig. 3(c) and Fig. 3(d) due to the increasing gravity component in the stream direction. In Fig. 3 the free surfaces are plotted at every plotting time step Δt=0.05.

In the next calculation, the evaporation is neglected by setting $\bar{E} = 0.5$. As known from the linear stability the initial evolution of the interface will be similar to the isothermal layer. The basic-state film thickness is h_0(=1). Fig. 4(a) shows free-surface configurations for $0 \leq t \leq 20$ with Δt=0.1. The surface becomes flat because there is not any instability effect acting on the layer. The stability is easily observed by the Fourier-spectral coefficients as in Fig. 4(b), where the fundamental magnitudes are exponentially decreased while the ±2 modes are slightly excited and then decayed out. Fig. 4(c) and Fig. 4(d) represent the free-surface deformations at β=15° and β=30°, respectively. In this case the K in (11) becomes an inverse Biot number and the thermocapillarity effect disappears at the horizontal static layer because the free-surface temperature has a constant value K. However, as the plane is inclined, the streamwise gravity force makes the layer drain into downward and the temperature on the perturbed surface is no longer in equilibrium with the vapor phase, that is, the heat transfer by the

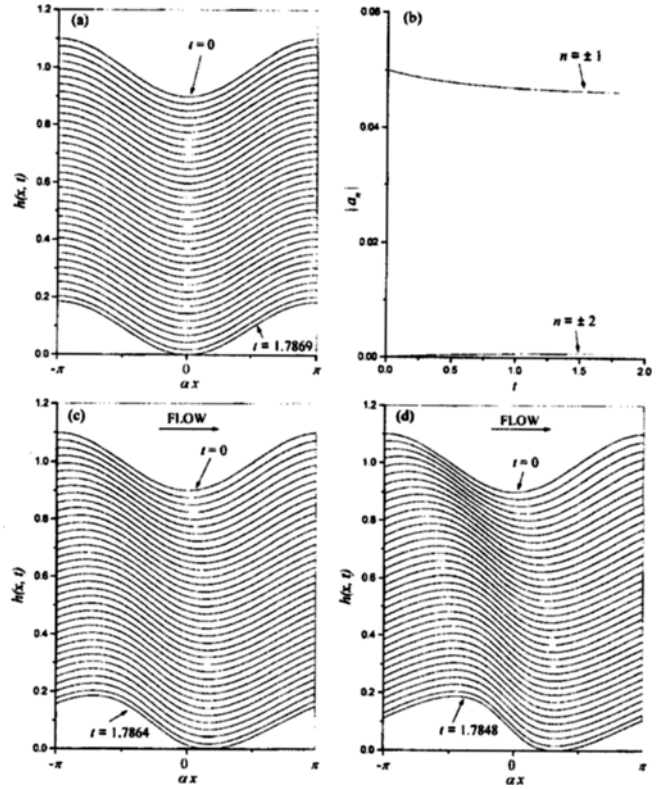

Fig. 3. Surface-wave behavior for the evaporating layer heated with a constant heat flux. α=0.8, $\bar{E}$ = 0.5, Fr^2=0.2, Pr=1.0, $\bar{D}$ = 0.1, K=0.2, M=100 and We=5. Free surfaces are plotted at every t=0.05.

(a) Free-surface configurations at β=0 and t_R=1.7869.
(b) Evolution of Fourier-spectral coefficients at β=0
(c) Free-surface configurations at β=15° and t_R=1.7864.
(d) Free-surface configurations at β=30° and t_R=1.7848.

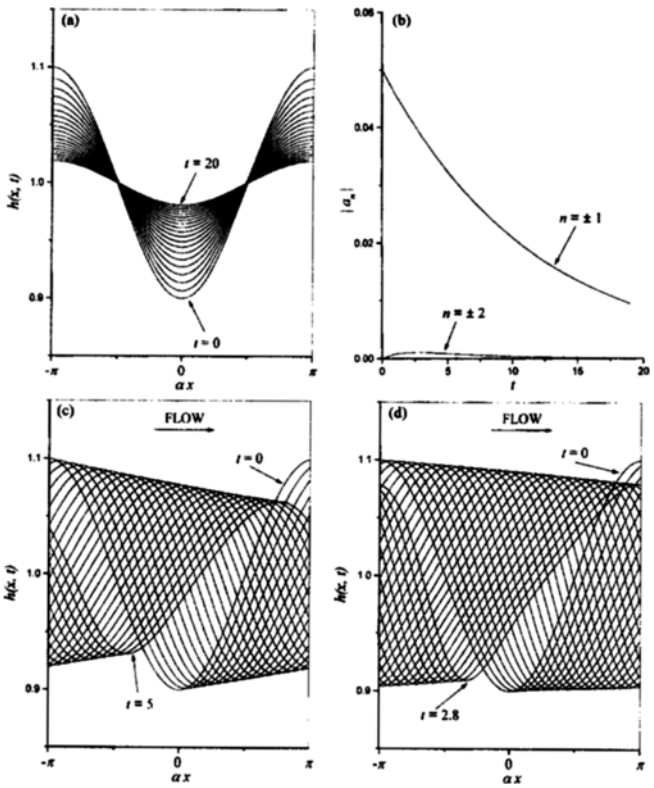

Fig. 4. Surface-wave behavior for the non-evaporating layer heated with a constant heat flux. α=0.8, $\bar{E}$ = 0, Fr^2=0.2, Pr=1.0, $\bar{D}$ = 0.1, K=0.2, M=100 and We=5. Free surfaces are plotted at every t=0.1 for (a) and (d), and at every t=0.2 for (c).

(a) Free-surface configurations at β=0 and $0 \le t \le 20$.
(b) Evolution of Fourier-spectral coefficients at β=0.
(c) Free-surface configurations at β=15° and $0 \le t \le 5$.
(d) Free-surface configurations at β=30° and $0 \le t \le 2.8$.

bulk fluid motion into the downstream becomes more significant than the heat output through the free surface. The surface temperature has a little lagged phase angle relative to the free-surface configuration and thus there is no thermocapillarity effect on the stability which has been observed if the evaporation effect is considered. Here, the stability aspect looks similar to that of an isothermal flow but it is noticeable that the phase speed of the interface has a higher value than the isothermal flow as one can see from C_0 in Eq. (25), where the temperature effect on the surface tension results in speeding up the surface waves into downwards.

2. At a Fixed Temperature Condition

Here, the evolution for the free-surface deformations has been computed to analyze the effect of the fixed temperature on the heated plane wall. As the linear stability analysis has shown the vapor recoil and the thermocapillarity effects are prominently destabilizing the system, one can expect these will also have influence on the nonlinear film evolution. To examine the nonlinear modal interactions of the free surfaces (20) has been numerically calculated with the initial condition (31) for the two cases, i.e., with or without the mass loss due to the evaporation. As in the previous case, three angles for the plane slope, i.e., β=0, β=15° and β=30°, are taken to interpret the combined inertial forces on the surface waves. In Fig. 5 the surface wave instabilities are computed with the fluid assumed volatile. The same values of the physical parameters are selected as in the constant heat flux case. Fig. 5(a) is for the static fluid resting on the horizontal plane, where the initial disturbance wavenumber is set 0.8 and each line is plotted at Δt= 0.05. As time marches the free surface becomes unstable and finally it ruptures at t_R=1.0845. Comparing with Fig. 3(a), one can see the dry-out time is faster under the same parametric values and the wave undulation has a steeper mode as in Fig. (a), where the cutoff wavenumber α_c and the maximum growth wavenumber α_m are 2.80 and 1.98, respectively. The instability behavior may be easily checked when we refer to the computed Fourier-spectral coefficients in Fig. 5(b). In the initial stage of instability the amplitude of the disturbance increases exponentially as we can guess from the linear stability theory, but soon it grows super-exponentially. With the angle β=15°, the wave propagation occurred from the streamwise gravity component worsens the instability as in Fig. 5(c), where α_c=2.83 and α_m=2.0. The location of the rupture is a little shifted into the downstream and the rear part of the wave travels faster than the front. The rupture time is much faster than that in Fig. 3(c) because the thermocapillarity and the vapor recoil act as significant instability factors. When the plate is more tilted to 30°,

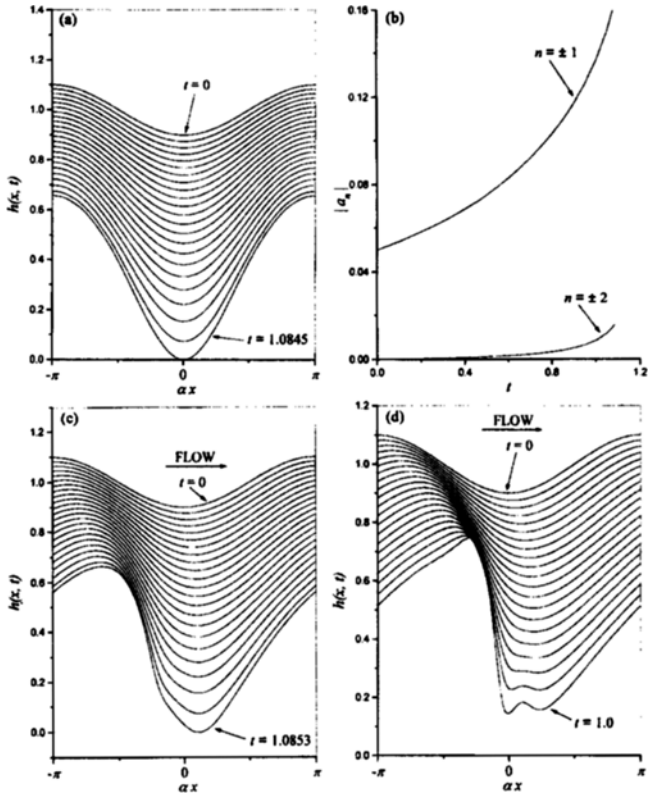

Fig. 5. Surface-wave behavior for the evaporating layer heated with a fixed temperature. α=0.8, $\bar{E}$ = 0.5, Fr^2=0.2, Pr=1.0, $\bar{D}$ = 0.1, K=0.2, M=100 and We=5. Free surfaces are plotted at every t=0.05.

(a) Free-surface configurations at β=0 and t_R=1.0845.
(b) Evolution of Fourier-spectral coefficients at β=0.
(c) Free-surface configurations at β=15° and t_R=1.0853.
(d) Free-surface configurations at β=30°.

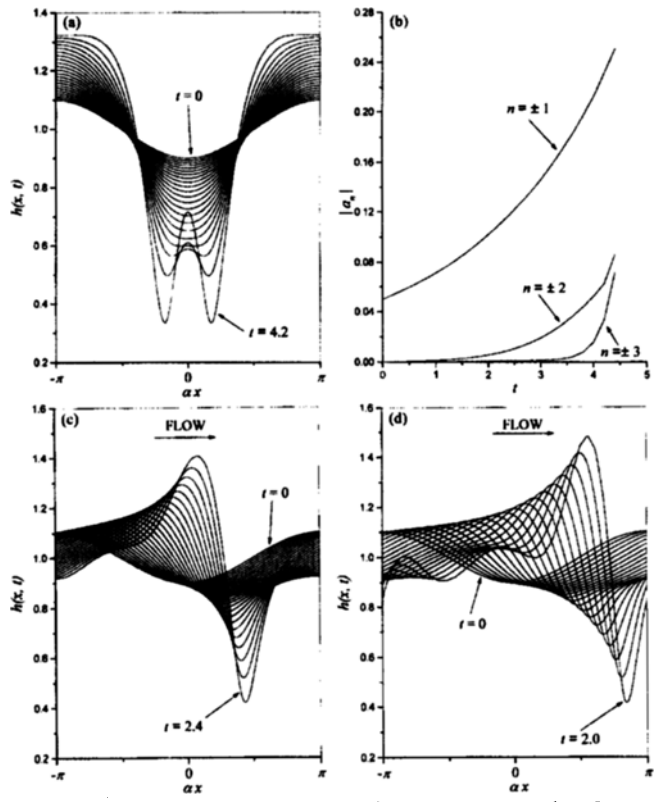

Fig. 6. Surface-wave behavior for the non-evaporating layer heated with a fixed temperature. α=0.8, $\bar{E}$ = 0, Fr^2=0.2, Pr=1.0, $\bar{D}$ = 0.1, K=0.2, M=100 and We=5. Free surfaces are plotted at every t=0.2 for (a) and at every t=0.1 for (c) and (d).

(a) Free-surface configurations at β=0 and $0 \le t \le 4.2$.
(b) Evolution of Fourier-spectral coefficients at β=0.
(c) Free-surface configurations at β=15° and $0 \le t \le 2.4$.
(d) Free-surface configurations at β=30° and $0 \le t \le 2.0$.

the disturbed wave travels faster than in the case of β=15°. Thus, under the instabilities from the increased gravity component combined with the thermocapillarity and the vapor recoil the rear part of the surface wave gets steeper and finally the wave is broken as in Fig. 5(d), where α_c=2.91 and α_m=2.06. Each line stands for the time increment of 0.05. As the wave gets thinner the heat transfer around the trough is so large that the layer is no longer in equilibrium with the vapor and so its thinning process is getting accelerated. The downward traveling speed of the trough slows because of its proximity of the bottom wall and hence the trough like a single fingertip gets flattened. The result is that the trough splits into two downward fingers as the line at t=1.0 in Fig. 5(d) reveals, which will eventually produce two dry spots. After this rupture we can expect that the advancing waves will over spread the dry spots before they are expanded. These rupturing and rewetting mechanisms will be alternating with each other before the layer is completely evaporated.

Next, the fluid is assumed nonvolatile to consider only the effect of thermocapillary instability. The same tilting angles are employed as in the previous calculations. For the purpose of comparisons the other physical and computational parameters are also kept having the same values as those at the constant heat flux case. When β=0°, the static layer becomes unstable to the initial small disturbance and shows more significant double-finger developments as in Fig. 6(a), where α_c=2.71, α_m=1.92 and the plotting time step Δt=0.2. In Fig. 6(b) the evolution of the Fourier-spectral coefficients is plotted upto n=±3. As the film gets unstable the higher modes are seen to be more excited. The free-surface configurations at β=15° and β=30° are plotted every Δt=0.1 in Fig. 6(c) and Fig. 6(d), respectively. As the slope gets larger the wave propagation speed is faster and the layer is confronted with a more serious instability, i.e., Fig. 6(d) shows dimples generating on the rear-wave site while the wave front gets steeper as time elapses. The surface-wave behaviors are much more stable than those with an extra evaporation effect embedded such as in Fig. 5. However, comparing these results with the ones obtained from the uniform heat flux case, this system is greatly unstable because the thermocapillarity acts as a significant instability factor for this boundary condition. Burelbach et al. [1988] reached the similar conclusion in a static thin film system. However, they did not find the thermocapillarity acted as a stabilizing factor at a constant heat flux condition because they derived the evolution equation only upto $O(\varepsilon)$.

CONCLUSIONS

To answer the questions concerning the stability of an evaporating thin liquid film heated under with either a constant heat flux or a fixed temperature, the nonlinear evolution equations for the film thickness have been derived by using the lubrication theory for the two cases. The approximation to the governing equations of motion and energy has been made upto order ε^2 for the constant heat-flux boundary condition so as to include the effects of thermocapillarity and vapor recoil for the volatile liquid whereas at a fixed wall temperature the derivation need not proceed to the order of magnitude because the thermal effects appear from $O(\varepsilon)$. By applying a small perturbation having a time-harmonic wave mode to a basic state which is a uniformly evaporating flat layer a linear stability analysis has been performed. At the constant heat-flux boundary condition the linearly unstable zone gets smaller in the $(\alpha-c_i)$ plane because the thermocapillarity and vapor recoil which exists only for the volatile fluid acts as stabilizing factors as time marches. This behavior can be explained by the temperature distribution of the deformed surface, that is, the temperature profile is similar to the surface-wave shape due to the characteristics of the given boundary condition. However, the effects of thermocapillarity and vapor recoil make the film evolution unstable at a constant wall temperature with the lapse of time because the crest of a disturbed wave has a colder temperature than the trough. To overcome the limit of the linear stability analysis which is only valid at the longwave approximation, nonlinear stability has been also performed with the aid of numerical computation. The computational domain is taken as a spatially periodic and the evolution equations are numerically solved by a Fourier-spectral method. At the inception of the computation the nonlinear outputs are well matched to the results from the linear stability analysis. The nonlinear stability analysis also reveals that the heated thin liquid-film flow below with a constant heat flux is much more stable than the flow at a fixed wall temperature because the thermocapillarity and vapor recoil act as stabilizing factors. If the liquid layer is nonvolatile, the thermocapillary effect only appears as a stabilizing thermal factor for the constant heat-flux case or as a destabilizing property for the constant wall-temperature system. Here several parametric physical values have been applied to the derived nonlinear film-evolution equations which govern the stability of the liquid layer subject to various coupled mechanisms. These include evaporation, thermocapillarity, vapor recoil, and viscous and inertial forces. Consequently, the flow subject to the constant heat flux can be marked as a much more stable system than the flow mechanism at a fixed wall-temperature condition.

ACKNOWLEDGMENT

This study was supported by the University of Seoul and the author gratefully acknowledges it.

NOMENCLATURE

C : capillary number ($=\gamma q_c h_N \sigma_0^{-1} k^{-1}$)
c : complex wave frequency
D : density ratio between liquid and vapor ($=3/2\ \rho^v \rho^{-1}$)
E : evaporation number ($=q_c h_N \rho^{-1} \nu^{-1} L_h^{-1}$)
$\bar{E}$: E/ε
Fr : Froude number ($=u_N/\sqrt{g h_N}$)
g : gravity [cm sec^{-2}]
h : dimensionless free-surface thickness
h_N : characteristic film thickness [cm]
h_0 : dimensionless basic-state film thickness
J : dimensionless mass flux
K : degree of non-equilibrium
k : thermal conductivity of the liquid [cal cm^{-1} sec^{-1} $°K^{-1}$]
L : characteristic length scale parallel to the plane [cm]
L_h : latent heat of evaporation [cal g^{-1}]
M : Marangoni number ($=\gamma q_c h_N 2^{-1} \rho^{-1} \kappa^{-1} u_N^{-1} k^{-1}$)
M_w : molecular weight [g/g mole]
N : number of modes in Fourier series
p : pressure [dyne/cm^2]
Pr : Prandtl number ($=\nu/\kappa$)
q_c : heat flux through the plane [cal $cm^{-2}sec^{-1}$]
Re : Reynolds number ($=u_N h_N \nu^{-1}$)
R_g : universal gas constant [cal g $mole^{-1}°K^{-1}$]
T : temperature [°K]
T_H : temperature on the plane [°K]
t : dimensionless time
u_N : characteristic unit of velocity in x direction [cm/sec]
u : dimensionless velocity component of x direction
v : dimensionless velocity component of y direction
We : Weber number ($=\sigma_0 \rho^{-1} u_N^{-2} h_N^{-1}$)
x : distance coordinate parallel to plane [cm]
y : distance coordinate perpendicular to plane [cm]

Greek Letters

α : wavenumber
α_{ac} : accommodation coefficient
β : inclination angle of plane with the horizontal [degree]
γ : temperature gradient of surface tension [dyne $cm^{-1}°K^{-1}$]
δ : small disturbance amplitude
ε : h_N/L
η : dimensionless film thickness perturbed from basic state
κ : thermal diffusivity [cm^2/sec]
Λ : dimensionless heat of evaporation
μ : fluid viscosity [g $cm^{-1}sec^{-1}$]
ν : kinematic viscosity [cm^2/sec]
ρ : fluid density [g/cm^3]
σ : surface tension [dyne/cm]
σ_0 : surface tension at T_s [dyne/cm]

Superscripts

I : interface between liquid and vapor
s : saturation temperature
v : vapor phase

Subscripts

c : critical value
i : imagninary part
m : maximum growth rate

r : real part
t : partial dervative with t
x : partial derivative with x
y : partial derivative with y

REFERENCES

Benjamin, T. B., "Wave Formation in Laminar Flow Down an Inclined Plane," *J. Fluid Mech.*, **2**, 554 (1957).

Benny, D. J., "Long Waves on Liquid Films," *J. Math. Phys.*, **45**, 150 (1966).

Burelbach, J. P., Bankoff, S. G. and Davis, S. H., "Nonlinear Stability of Evaporating/Condensing Liquid Films," *J. Fluid Mech.*, **195**, 463 (1988).

Chang, H.-C., "Onset of Nonlinear Waves on Falling Films," *Phys. Fluids A*, **1**(8), 1314 (1989).

Delhaye, J. M., "Jump Conditions and Entropy Sources in Two Phase Systems: Local Instant Formulation," *Int. J. Multiphase Flow*, **1**, 395 (1974).

Gjevik, B., "Occurrence of Finite-Amplitude Surface Waves on Falling Liquid Films," *Phys. Fluids*, **13**, 1918 (1970).

Joo, S. W., Davis, S. H. and Bankoff, S. G., "Long-wave Instabilities of Heated Falling Films: Two-dimensional Theory of Uniform Layers," *J. Fluid Mech.*, **230**, 117 (1991).

Kim, H., Bankoff, S. G. and Miksis, M. J., "Electrostatic Field Effects on a Rotating Liquid Film Conical Radiator," *AIAA J. Propulsion and Power*, **9**, 245 (1993).

Kim, H., Bankoff, S. G. and Miksis, M. J., "The Cylindrical Electrostatic Liquid Film Radiator for Heat Rejection in Space," *J. Heat Transfer*, **116**, 986 (1994).

Kim, H., Bankoff, S. G. and Miksis, M. J., "The Effect of an Electrostatic Field on Film Flow Down an Inclined Plane," *Phys. Fluids A*, **4**, 2117 (1992).

Kim, H., "Long-Wave Instabilities of Film Flow under an Electrostatic Field: Two-Dimensional Disturbance Theory," *Korean J. Chem. Eng.*, **14**, 41 (1997).

Lin, S.-P., "Finite Amplitude Side-Band Stability of a Viscous Film," *J. Fluid Mech.*, **63**, 417 (1974).

Palmer, H. J., "The Hydrodynamic Stability of Rapidly Evaporating Liquids at Reduced Pressure," *J. Fluid Mech.*, **75**, 487 (1976).

Yih, C.-S., "Stability of Liquid Flow Down an Inclined Plane," *Phys. Fluids*, **5**, 321 (1963).